

PRECISION POINTING FOR THE WIDE-FIELD INFRARED SURVEY TELESCOPE (WFIRST)

Eric T. Stoneking^{*}, Oscar C. Hsu[†], and Gary Welter[°]

The Wide-Field Infrared Survey Telescope (WFIRST) mission, scheduled for a mid-2020's launch, is currently in its definition phase. The mission is designed to investigate essential questions in the areas of dark energy, exoplanets, and infrared astrophysics. WFIRST will use a 2.4-meter primary telescope (same size as the Hubble Space Telescope's primary mirror) and two instruments: the Wide Field Instrument (WFI) and the Coronagraph Instrument (CGI). In order to address the critical science requirements, the WFIRST mission will conduct large-scale surveys of the infrared sky, requiring both agility and precision pointing (11.6 milli-arcsec stability, 14 milli-arcsec jitter). This paper describes some of the challenges this mission profile presents to the Guidance, Navigation, and Control (GNC) subsystem, and some of the design elements chosen to accommodate those challenges. The high-galactic-latitude survey is characterized by 3-minute observations separated by slews ranging from 0.025 deg to 0.8 deg. The need for observation efficiency drives the slew and settle process to be as rapid as possible. A description of the shaped slew profile chosen to minimize excitation of structural oscillation, and the handoff from star tracker-gyro control to fine guidance sensor control is detailed. Also presented is the fine guidance sensor (FGS), which is integral with the primary instrument (WFI). The FGS is capable of tracking up to 18 guide stars, enabling robust FGS acquisition and precision pointing. To avoid excitation of observatory structural jitter, reaction wheel speeds are operationally maintained within set limits. In addition, the wheel balance law is designed to maintain 1-Hz separation between the wheel speeds to avoid reinforcing jitter excitation at any particular frequency. The wheel balance law and operational implications are described. Finally, the candidate GNC hardware suite needed to meet the requirements of the mission is presented.

INTRODUCTION

The Wide-Field Infrared Survey Telescope (WFIRST) mission, scheduled for a mid-2020's launch, is currently in its definition phase. The mission is designed to investigate essential

^{*} Senior Aerospace Engineer, Attitude Control Systems Engineering Branch, NASA Goddard Space Flight Center, Code 591, Greenbelt MD 20771.

[†] Aerospace Engineer, Attitude Control Systems Engineering Branch, NASA Goddard Space Flight Center, Code 591, Greenbelt MD 20771.

[°] Aerospace Technologist, Flight Software Branch, NASA Goddard Space Flight Center, Code 582, Greenbelt MD 20771

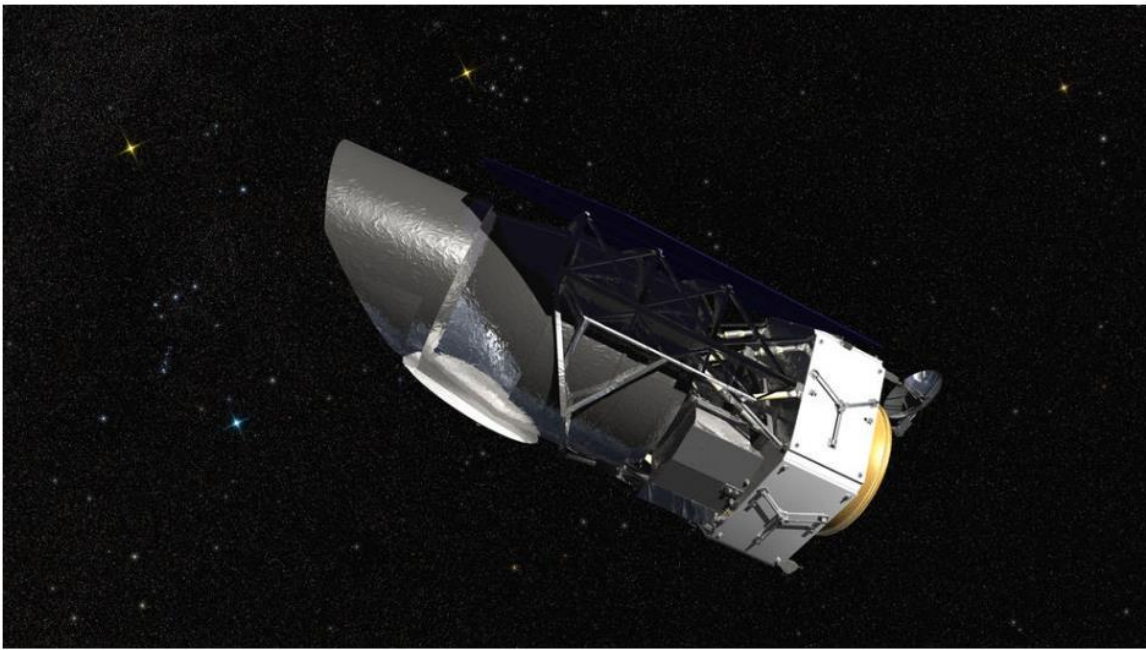


Figure 1. WFIRST Observatory¹

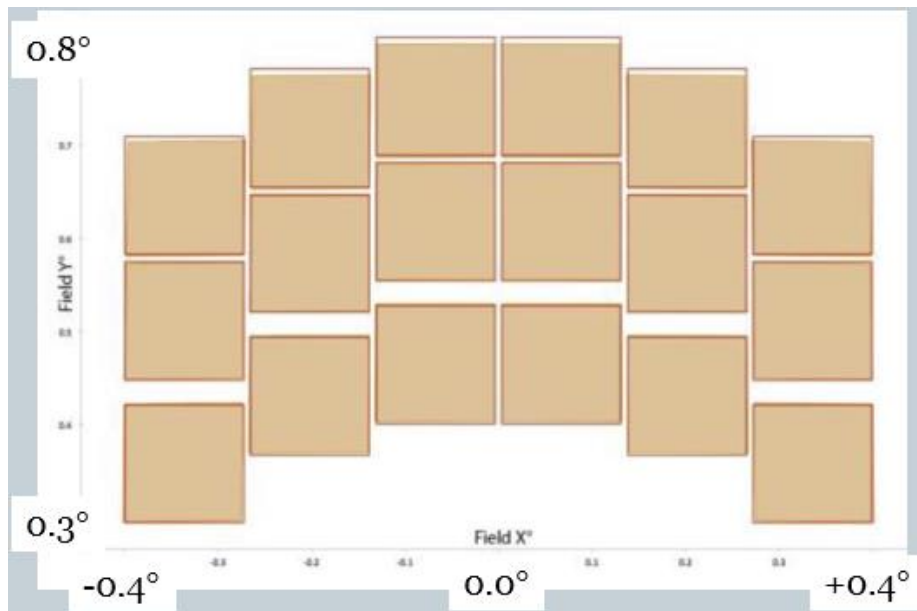


Figure 2. The WFIRST Field of View is over 200x that of Hubble's Wide Field Camera 3; Image shows relative size and position of the 18 WFI detectors²

questions in the areas of dark energy, exoplanets, and infrared astrophysics. As seen in Figure 1, WFIRST will use a 2.4-meter primary telescope (the same size as the Hubble Space Telescope's primary mirror) and two instruments: the Wide Field Instrument (WFI) and the Coronagraph Instrument (CGI). In order to address the critical science requirements, the WFIRST mission will conduct large-scale surveys of the infrared sky, requiring both agility and precision pointing (11.6 milli-arcsec stability over an exposure, 14 milli-arcsec jitter). This paper describes some of the

challenges this mission profile presents to the Guidance, Navigation, and Control (GNC) subsystem, and some of the design elements chosen to accommodate those challenges.

DESCRIPTION OF FINE GUIDANCE SENSOR

The WFI uses 18 HAWAII-4RG 4K×4K detectors⁷ (Figure 2) to collect science data, each pixel having a linear pitch of ~110 milli-arcsec on the sky. Note that the pixel size is about an order of magnitude larger than the required pointing precision. Each detector has the capability to read the data from a small selected guide window separately from the science data stream. This capability is used to implement a Fine Guidance Sensor (FGS) integral to the WFI. Up to 18 guide stars are tracked, centroided and combined to obtain roll, pitch, and yaw attitude error signals. Angular rate measurements are derived from the attitude measurements, making the FGS the sole attitude sensor for science-quality pointing.

The FGS will be operated in two modes. During imaging surveys, the FGS centroided on the images of the guide stars. While the detector readout frame time is approximately five seconds, the nominal 16×16 image mode guide window exposure time is ~0.17 second. WFI science images are acquired using one of six filters ([Z: 0.76-0.98], [Y: 0.93-1.19], [J: 1.13-1.45], [H: 1.38-1.77], [F: 1.68-2.00], & [W: 0.97-2.00] μm). The FGS star images are acquired using the same filters as the science data, with the implication that there are six different point spread functions (PSFs) that can be used. Note that the half-widths of the PSFs ($\sim 1.2 \lambda/D$) range between ~0.82 pixel (Z) to 1.73 pixels (F). See Figure 3 for a sample simulated PSF. Two dimensional centroiding is done by first finding the brightest pixel within the 16×16 guide window, and then centroiding within an N×N box centered on that brightest pixel. Using N = 5 provides good results in the analysis. The chosen value for N is a good compromise between the faint guide stars to discard pixels that primarily contain noise while including the most important pixels with true signal. Two centroiding algorithms have been studied for use within the N×N box: (a) simple first moment centroiding with each pixel weighted by its signal, and (b) a lowest-non-zero frequency Discrete Fourier Transform in each dimension with the centroid determined from the transform phase shift. The latter algorithm is the same as that used by the James Webb Space Telescope FGS team; it is more robust to noise than simple first moment centroiding. Both algorithms are subject to a systematic pixelation effect that leaves the estimated centroid offset from truth in each dimension by an amount that is approximately proportional to $\sin(2\pi\Delta)$, where Δ is the fraction of a pixel width that the true star location is separated from the center of the central pixel. The amplitude of the offset is dependent on the filter, box size, and centroiding algorithm. For the Z filter, the amplitude of the offset is ~0.1 pixel, thus it is significant relative to the required accuracy. Applying this correction is the last step in centroiding. The set of centroids are then combined with catalog star coordinates to estimate observatory attitude. Simulations show image-mode pitch-yaw measurement filter-dependent precision between 1.0 and 4.4 milli-arcsec, root-mean-square (RMS), assuming 16 K0V guide stars at the dim end of the guide star H(AB) magnitude range (14.5-17).

During spectroscopic surveys, the guide star images are spread in one dimension over about eight hundred pixels, greatly reducing the photon flux per pixel and requiring a modified centroiding method for the along-spectrum direction – indeed, a redefinition of “centroid” for that direction. (Centroiding for the cross-spectrum direction remains much as described for image mode.) A single filter will be used for spectroscopy, one that has fairly flat transmittance (~0.95) over a range of about 1.0-1.9 μm . Spectral spread is obtained using a grism, with the spectrum

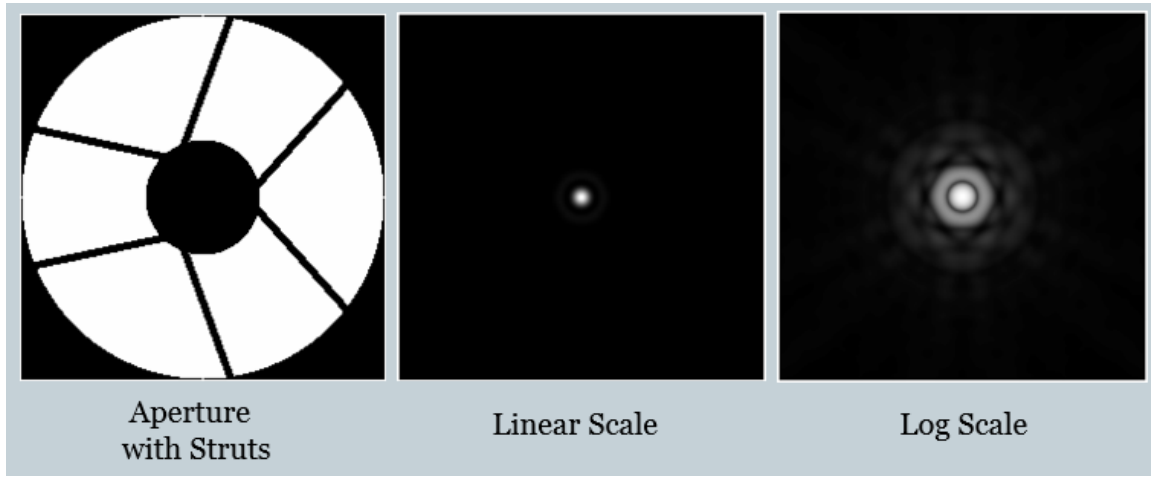


Figure 3. FGS Imaging Point Spread Function

High resolution simulation: 128-to-1 linear scale, box equivalent to 17x17 Pixels;
 Z filter; Black body spectrum with $T_{\text{Eff}} = 9700 \text{ K}$ ($\sim \text{A0V}$ spectral type);
 Perfect imaging (i.e., no defocus, no wavefront error, no high-frequency jitter)

observed in first order and with dispersion of $\sim 1.085 \text{ nm/pixel}$. See Figure 4 for a sample simulated partial spectrum near the $1\text{-}\mu\text{m}$ edge. The “centroiding” method currently under study is to fit a data set obtained using a 16×32 guide window to a model of a selected end of the spectrum (nominally, the $1\text{-}\mu\text{m}$ end, which we assume for the rest of the discussion). An N -pixel wide horizontal band ($N \sim 3$) centered on the spectrum is first compressed into one dimension. The weight-free loss function chosen for minimization is given by

$$J(c_E, G_R) = \sum_i (S_i - G_R M(c_i; c_E, \delta_R))^2 \quad (1)$$

c_E = the along-spectrum “centroid” coordinate (details defined below)

G_R = estimated flux per pixel at a reference displacement δ_R from c_E

S_i = measured spectrum flux at i -th column coordinate

$M(c_i; c_E, \delta_R)$ = normalized spectrum model

c_i = i -th column coordinate (units: pixels)

The pair (c_E, G_R) is our two-element state vector. The normalized model, consists of two parts: the edge shape, $E(c)$, and the grism blaze function, $B(c)$, where c is the along-spectrum column coordinate in pixels:

$$M(c; c_E, \delta_R) = E(c; c_E) B(c; c_E, \delta_R) \quad (2.1)$$

$$E(c; c_E) = \frac{1}{2} (1 + \tanh(a_E (c - c_E))) \quad (2.2)$$

$$B(c; c_E, \delta_R) = 1 + s_B (c - (c_E + \delta_R)) \quad (2.3)$$

Use of the functional form for $E(c)$ specified in equation 2.2 is convenient and close enough. The parameter a_E is determined by fitting $E(c; c_E)$ to a high-resolution model of the spectrum edge shape based on knowledge of filter edge shape, the stellar undispersed PSF, and dispersion of the PSF through the filter edge wavelengths; we find $a_E \approx 0.22$. The grism blaze function is fairly linear and steep near $1 \mu\text{m}$; with δ_R set to 20 pixels, the parameter s_B is $\sim 0.0097/\text{pixel}$. Actually, one also needs a small correction to s_B based on guide star spectral type; this correction ranges from -0.0023 to -0.0002 for A0V to M0V stars, respectively. We use an iterative algorithm to minimize J and determine c_E . During track mode, after one has already established near-proper



Figure 4. FGS Spectroscopy “Blue” Spectral Edge

High resolution simulation: 64-to-1 linear scale, box equivalent to 18x36 Pixels;

Black body spectrum with $T_{\text{Eff}} = 5300 \text{ K}$ ($\sim \text{K0V}$ spectral type);

Perfect imaging (i.e., no defocus, no wavefront error, no high-frequency jitter)

positioning of the spectrum edge, the algorithm only requires a few iterations to converge. With a set of centroids determined, one solves for an attitude estimate as before. In spectroscopic mode, the stability requirements are relaxed to 100 mas in the along-spectrum direction. Simulations show that this performance is attainable assuming at least 3 guide stars with flux at 1- μm equivalent to or brighter than a K0V star with H(AB) magnitude 12, read noise of 15 electrons, and exposure time of ~ 0.25 second.

ACQUISITION OF FINE GUIDANCE SENSOR

WFIRST's operations are dominated by surveys, routinely visiting hundreds of targets per day. To meet the survey coverage requirements in its six-year mission lifespan, slews must be rapid. During slews, the WFI detectors are put into a standby mode to protect them from bright stars, rendering the FGS inoperative, so star tracker (ST) and inertial reference unit (IRU) measurements are used for attitude determination during slews. The handoff from ST-IRU to FGS-based control must be rapid and robust to maintain the survey operational tempo. A separate settle mode is employed to handle this transition.

Settle mode is entered when the slew reference attitude has reached the new target attitude. The true attitude differs from the reference attitude due to measurement and control errors. The FGS guide windows are enabled and placed at the expected location of each guide star, with a goal of one guide star per detector in imaging mode. For acquisition, each guide window size is 64×64 pixels, spanning ± 3.5 arcsec and enveloping the star tracker noise-equivalent angle of 2 arcsec RMS. It is assumed that star tracker-to-FGS alignments will be calibrated often, so that systematic star tracker errors may be neglected. Also, it is not required that the acquisition window envelope the star tracker 3-sigma noise-equivalent angle (NEA) because it is not necessary for every guide star to be acquired on the first measurement cycle of the search. It is acceptable to initially obtain only a subset of the 18 guide stars, using these to improve the search for the

rest. And it is acceptable to loiter for a short time if needed for the star tracker-based control to settle to within its RMS accuracy.

A pattern matching algorithm is used to test each candidate guide star and confirm proper identification. After sufficiently many confirmed guide stars have been found, they are used to compute an attitude solution. When enough guide stars have been found, all guide windows are reduced to the nominal tracking size of 16×16 pixels, and any guide window not tracking a valid star is reinitialized. This step makes the acquisition process robust to near-neighbor stars and other catalog-related problems, and allows the GNC subsystem to begin tracking on FGS measurements quickly while the remaining guide windows continue to search for stars. To be robust to the possibility that the attitude may not be fully settled at this handoff to FGS-based control, the guide windows are required to be capable of moving on the detectors to maintain track on their guide stars.

Once under FGS control, the attitude is stabilized. For some science operations, the absolute pointing requirement (relative to the guide star catalog) may be on the sub-pixel level ("precise" pointing). For other survey operations, the absolute pointing requirement is relatively relaxed, as long as the pointing stability is still at the 11.6-milli-arcsec requirement ("stable" pointing). As it may be quicker to achieve stable pointing than to converge to precise pointing, different criteria for the transition from Settle mode to Inertial Hold mode are used in the two cases, in the interest of observation efficiency.

The discussion in the preceding three paragraphs pertains to imaging mode. It generally pertains in spectroscopy mode as well, with a few modifications. First, the regions of the sky in which spectroscopy can be done must have sufficiently low star density that spectra won't overlap. Furthermore, guiding on spectrum edges requires the use of brighter stars. The implication for spectroscopy field guide star availability is that only a few (~ 3) guide stars are expected to be available across the whole set of 18 detectors for any given pointing. Pattern matching will probably be trivially simple; with so few bright stars, the probability of a star that is not the intended guide star being seen is negligible. Also, we leverage the spectroscopy mode asymmetry by initially targeting a position within the spread spectrum, a few acquisition guide window widths long-wards of the $1\text{-}\mu\text{m}$ "blue" edge. This allows an initial 1-D acquisition in the vertical direction followed by walking rapidly (say, in half window steps) in the horizontal direction to find the "blue" edge. There is a complication that starting the spectral mode centroiding algorithm with the spectral edge randomly placed in the window requires extra iterations to converge, even with a relatively coarse convergence limit. Our current estimate for the expectation time for centroiding of a single randomly placed spectral edge within the left-most two-thirds of a 64-pixel-wide acquisition window on a LEON3 processor is $\sim 8\text{ ms}^8$. This assumes pre-computation of the normalized spectrum, $M(c)$, at high-resolution after uplink of its defining parameters a_E and δ_R ; in-line computation of $M(c)$ during centroiding increases the estimated time to $\sim 30\text{ ms}$. The latter is a bit tight if we need to fit all centroiding computations for (say) four stars within an acquisition exposure time period of $\sim 250\text{ ms}$; that would leave us with a central processing unit (CPU) margin at this fairly early stage of only 50%. But during acquisition it may well suffice to just use one or two stars. We also have some possible trading to do between computer memory for pre-computation of $M(c)$ vs. CPU time for in-line computation ... vs. getting a bigger boat.

SHAPED SLEW PROFILE

To support a survey operational tempo, the slew between successive targets must be rapid, but must at the same time avoid exciting poorly-damped structural or slosh oscillations that could

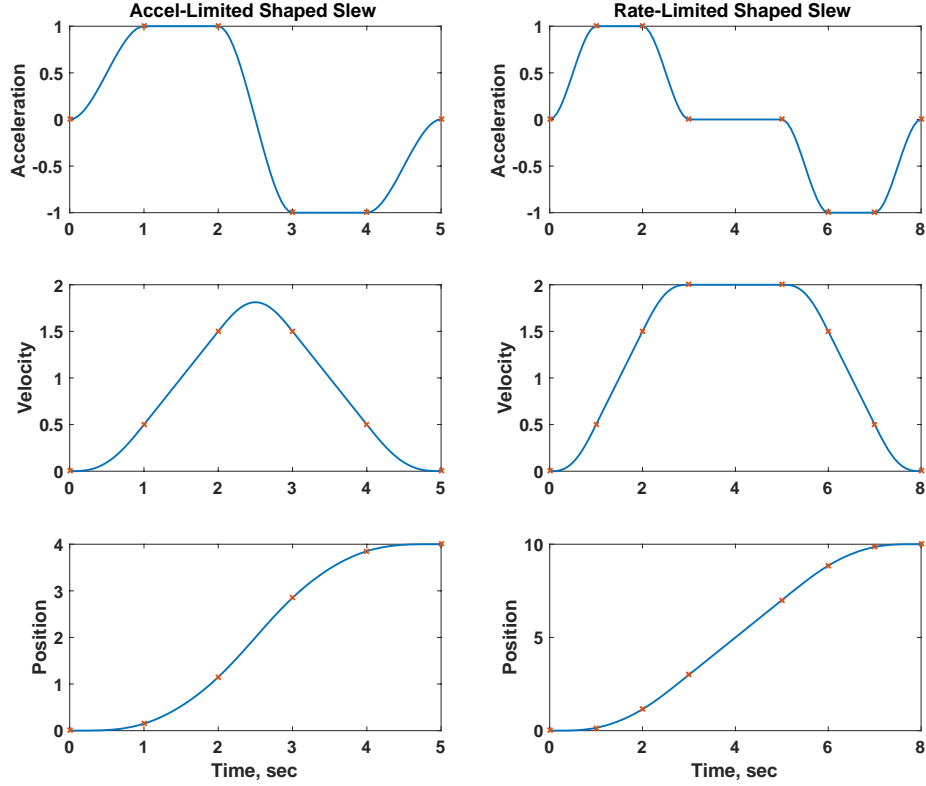


Figure 5. Shaped Slew Profiles

adversely affect settling time. To achieve this, a shaped profile is computed onboard for each slew. The profile is acceleration-limited for slews below 6.5 deg, and rate-limited for longer slews. To avoid discontinuities that may excite structural oscillations, the acceleration profile is shaped using the cubic curve

$$f(u) = 3u^2 - 2u^3 \quad (4)$$

In all non-contingency operations, the telescope boresight axis (the observatory +X axis) is maintained at all times within a field of regard (FoR) defined as the region on the sky between 54 deg and 126 deg from the Sun. The near-Sun constraint is especially critical, as the telescope optics may suffer catastrophic damage if exposed to direct sunlight. A safety buffer is defined for contingencies, but for all nominal operations, the +X axis is required to be kept within the FoR. For this reason, an eigenaxis slew profile is not appropriate. This is illustrated in Figure 6, which shows an eigenaxis slew that rotates 180 deg about Z and 30 deg about X. The trace of the +X axis (shown in red) travels through the Sun exclusion zone (in gray). Instead, the slew is decomposed into three single-axis slews, using Euler axes referenced to the FoR frame. These three slews are executed concurrently, with the two shorter components scaled in time to match the duration of the longest component. Figure 7 shows this per-axis slew profile, using the same start and ending attitudes as the eigen-axis case, but maintaining the +X axis within the FoR throughout the slew. Since the Euler angles used in the slew are referenced to the FoR reference frame, the trace of the +X axis is guaranteed to lie within the FoR as long as both its start and end locations do so.

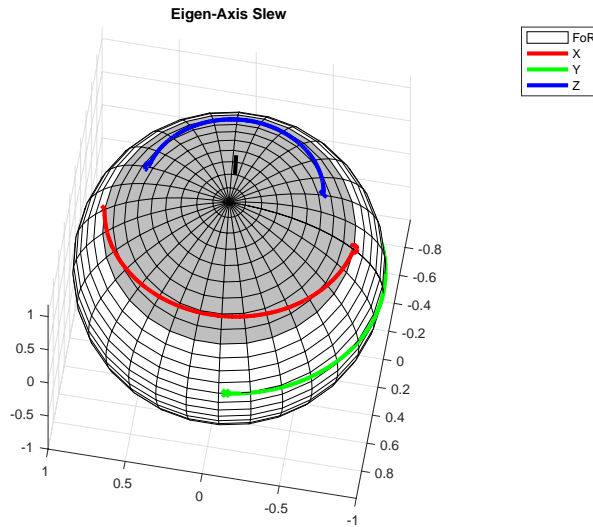


Figure 6. X-axis Trace may violate Field of Regard during Eigenaxis Slew

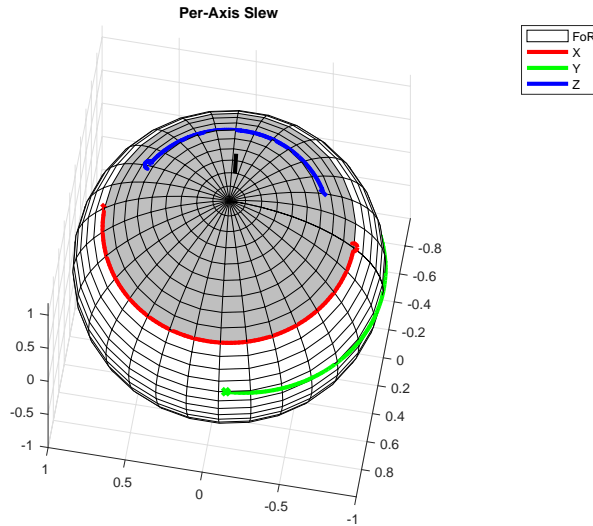


Figure 7. X-axis Trace is always within Field of Regard during Per-axis Slew

WHEEL BALANCE NULLSPACE CONTROL LAW

Like many spacecraft, WFIRST has more than three wheels for fault tolerance. While more than three wheels are available, there are $(N-3)$ additional degrees of freedom (DOF) in the nullspace of the projection of the wheel torque space onto the spacecraft body torque space. A "wheel balance" control law is implemented to accomplish wheel-related objectives in parallel with the wheels' primary task as torque actuators. This section describes a single-DOF balance law, corresponding to a four-wheel architecture. WFIRST is in the process of transitioning to a six-wheel architecture, which will allow the use of up to three DOF in the wheel balance law, but that has not yet been implemented. For the present, the use of a single degree of freedom to achieve three objectives is described.

First, all wheels are nudged toward zero speed, in proportion to their current speed. This is a common balance law, having the effect of keeping the wheel speeds grouped together.

The second objective is more unusual. To avoid the contributions to wheel-induced jitter from reinforcing each other, it is desirable to keep the wheel speeds separated by 1 Hz or more. There are not enough degrees of freedom to control the mutual separation of all pairs, so some of this objective must be managed by setting the initial wheel speeds at each momentum unload. But the wheel balance law may be used to push certain pairs of wheels away from each other. For example, with a null vector of $Nw = [+1 -1 +1 -1]$, wheels 1 and 3 cannot be influenced independently, nor can wheels 2 and 4. This is because the corresponding components of the null vector are equal. But the pairs (1,3) and (2,4) may be pushed toward or away from each other.

The third objective is to minimize attitude excursions due to zero speed crossings. To avoid structural excitation, the wheel speed operating range (during science observations) is limited to less than 40 Hz (2400 rpm) in absolute value. In order to maximize the interval between momentum unloading events, the wheel speed range is two-sided: -40 to +40 Hz, allowing the wheels to pass through zero speed. Wheel stiction at zero speed causes a transient disturbance torque which will temporarily degrade pointing performance. To minimize this degradation, it is desired to "push through" zero speed quickly, not loitering at very low speed. This is done using an additional term in the wheel balance law.

For a four-wheel configuration, the wheel nullspace has only one dimension, so it is not possible to satisfy all objectives independently at the same time. The resulting wheel balance law is a weighted sum of the three contributions. The zero-speed term is only active in a limited speed range, and is weighted relatively heavily. The "stay together" and "keep apart" terms are naturally antagonistic, striking a balance.

Figure 8 shows the absolute magnitudes of wheel momenta for a steady inertial hold simulation case. The secular drift is due to external solar radiation pressure torque. The wheel momenta are separated by 3 Nms to satisfy the 1-Hz separation requirement. As each wheel approaches zero, it is quickly pushed through, then loiters at a constant speed until the external torque imparts enough momentum on the system to allow the wheel to resume its normal trend. The wheel

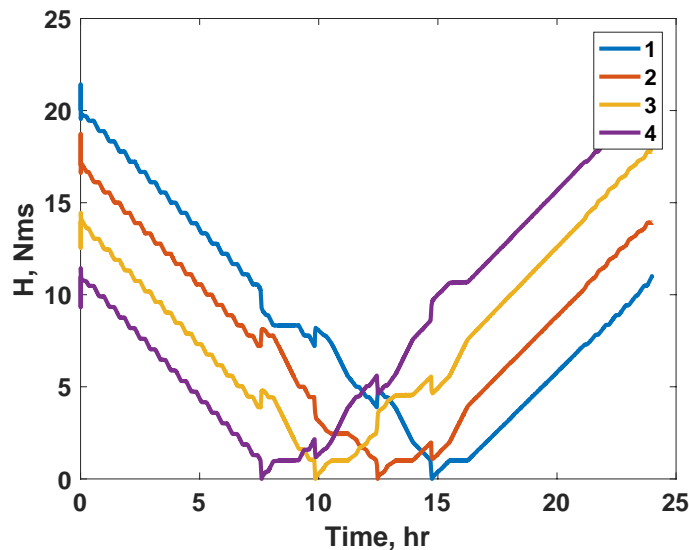


Figure 8. Typical Wheel Speed Profile During Inertial Hold

speeds are spaced widely enough so that only one wheel is in this near-zero condition at a time.

GNC HARDWARE SUITE

The GNC hardware suite to support the WFIRST mission consists of both a sensor suite and an actuator suite of hardware. The sensor suite consists of coarse sun sensors, inertial reference unit (IRU), star trackers, and fine guidance sensor. The actuator suite consists of thrusters and reaction wheels.

Coarse sun sensors will be used for coarse pointing of the observatory to ensure that the observatory is both power and thermally safe whenever in Safe mode. The sensors will be placed to provide $4\text{-}\pi$ steradian coverage, and each location will have two sensing elements to provide single fault tolerance. The assumption is that each sensor will have full field of view of $2\text{-}\pi$ steradian.

The IRU will be used for measuring the observatory angular rate in three axes. The IRU is used in the observatory safe mode for maintaining a power-safe and thermally safe environment, in thruster based modes as the primary attitude sensor for maintain pointing, and as previously mentioned, in the fine-pointing modes. In particular, the IRU has primary attitude estimation responsibility during slews between science targets. Angle random walk (ARW) is the driving error source for attitude estimation during slews, especially for large (>10 deg) slews. For this reason, ARW will be a key discriminator in the selection of an IRU for WFIRST. Angular rate sensing will need to be single-fault tolerant and WFIRST is considering either the use of an internally redundant IRU or multiple IRUs to achieve the single-fault tolerance requirement.

Star trackers will be used for measuring the attitude of the observatory in three axes. The star sensor is primarily used to transition the observatory between survey targets and when the fine guidance sensor is not in use. Attitude measurements by the star sensor will need to also be single fault tolerant. In order to achieve single fault tolerance, the observatory will need 3 optical heads or 3 stand-alone autonomous star sensors. The star sensor system needs to have a NEA of 2 arcseconds 1-sigma.

The FGS is part of the WFI and used to achieve the fine pointing necessary to perform the WFIRST Science mission. The FGS is composed of 18 guide windows, one on each science detector, that can be placed anywhere on each science detector. The FGS will determine the centroid of a guide star within each guide window and provide the centroid information to the GNC software. The FGS is single fault tolerant with the use of 18 possible detectors and redundant electronics.

The propulsion system will use a monopropellant (hydrazine) fuel in a blowdown mode. The system will utilize sixteen 5-N class thrusters and eight 22-N class thrusters for course correction maneuvers, station-keeping maneuvers, and momentum unload maneuvers. The propulsion system is not designed for use in precision pointing of the observatory or for the rapid slews needed by the observation campaign. Figure 9 shows the thruster thrust axes and preliminary plume avoidance cones.

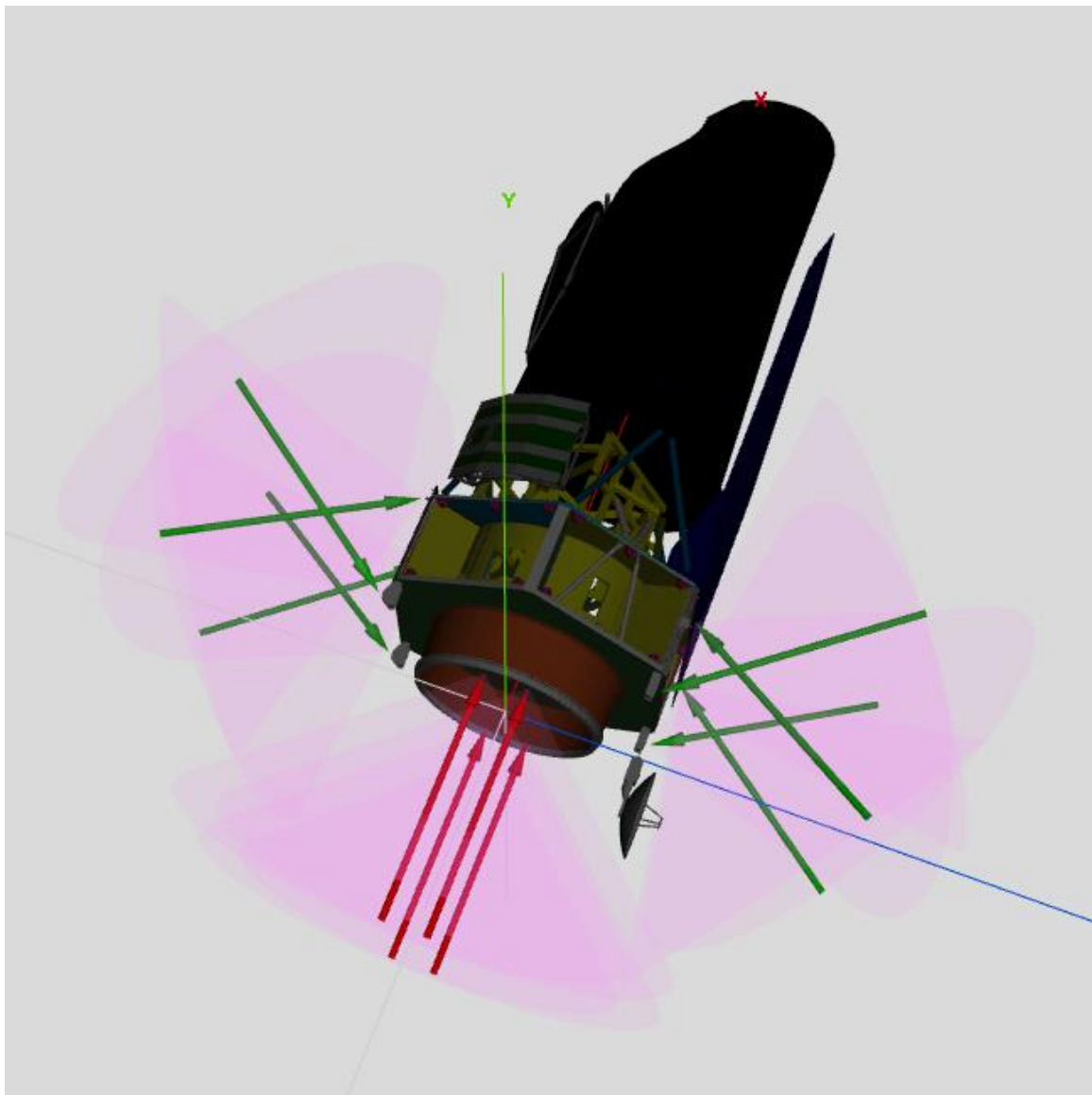


Figure 9. Thruster Layout, Showing Thrust Axes and Plume Keepout Cones

The reaction wheel assembly will be used for achieving the fine pointing requirement and the rapid slews needed for the observation campaign. Due to the size and mass distribution of the WFIRST observatory, high-torque wheels with large momentum storage capacity are needed. Based on current understanding of the most challenging agility requirements, WFIRST is in the process of moving to a configuration of six reaction wheels, each with the capability to provide 0.65 N-m of torque and 48 Nms of momentum at 3100 RPM. Candidate wheels are in the process of being identified. WFIRST is concerned about higher wheel speeds causing jitter issues during science observations. A six-wheel configuration would meet all agility requirements in the case of a single wheel failure. It would of course tolerate up to three wheel failures with progressively degraded performance, but there is no requirement for that capability. Figure 10 shows a six-wheel torque envelope, a five-wheel envelope obtained by failure of one wheel (both in yellow), and the octahedron representing the driving torque requirement (dark gray).

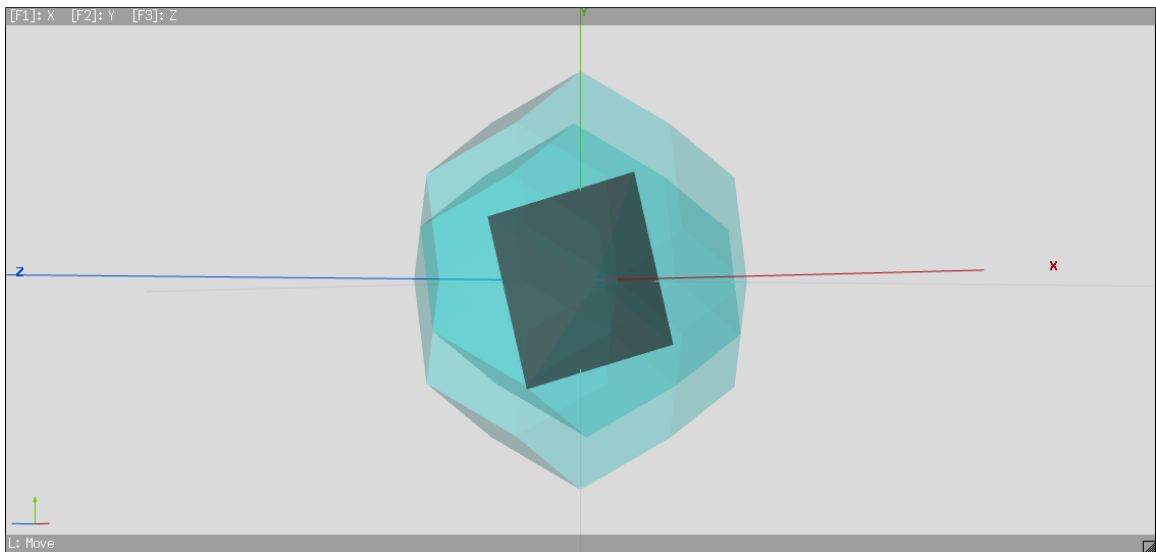


Figure 10. Six-Wheel Torque/Momentum Envelope

CONCLUSION

The WFIRST mission presents a unique combination of challenges to the GNC subsystem. Its attitude stability and jitter requirements are of the same order of magnitude as the Hubble and James Webb Space Telescopes, but the field of view is much larger, and the survey-driven pointing profile is much more agile, placing a premium on rapid slewing and settling, and rapid acquisition of the fine guidance sensor. To meet the accuracy requirements, the FGS is integral with the WFI detector, using up to 18 guide stars to provide robust target acquisition, three-axis pointing measurements and to reduce the aggregate measurement noise. The slew profile is designed to avoid excitation of structural oscillation and to maintain the telescope boresight axis within the science field of regard throughout the slew. In order to manage wheel-induced jitter during observations, the wheel nullspace law is used to maintain wheel speed separation (as much as that is possible) and to minimize disturbances due to zero-speed crossings.

Although the final GNC hardware suite has not yet been selected, the general component complement and capabilities have been outlined. Aside from the integral fine guidance sensor, the remaining GNC hardware will be acquired as off-the-shelf components. Identification of a reaction wheel model (and quantity) that meets WFIRST's torque and momentum requirements is an ongoing activity.

ACKNOWLEDGEMENTS

We acknowledge conversations with Jeff Kruk regarding the use of WFI guide windows in FGS mode. He provided valuable insights regarding observatory throughput of star light in both imaging and spectroscopic modes. He also provided independent calculations of the expected precision of FGS centroid calculations, against which we compared our own calculations. We acknowledge conversations with Alden Jurling regarding efficient methods for 2-D Fourier transform computations for broadband point spread function generation, in particular the discussion in Section 5.3.4 of his PhD thesis (see reference 6 below) regarding the separable DFT matrix triple product method.

REFERENCES

1. For Figure 1, see: <https://www.nasa.gov/press-release/nasa-introduces-new-wider-set-of-eyes-on-the-universe>
2. For Figure 2 and related discussion of the WFIRST field-of-view layout, see: "Optical Design of the WFIRST-AFTA Wide Field Instrument" by Pasquale et al (SPIE-OSA 929305-1), SPIE-OSA/ Vol. 9293, 2014
3. Kruk, J., Noise Equivalent Angle Estimates: Using the WFIRST Wide-Field Imager as a Fine Guidance Sensor when doing broad-band imaging, NASA/GSFC Technical Memo, October 22, 2014
4. Kruk, J., Guiding On Grism Images – v2, Presentation to the WFIRST WFI Ops Working Group, September 22, 2016
5. Hirata, C., Science Implications of GRS Guiding without the Aux Guider: A First Look, Presentation to the WFIRST WFI Ops Working Group, September 1, 2016
6. Jurling, A., Advances in Algorithms for Image Based Wavefront Sensing, PhD Thesis, The Institute of Optics Arts, Sciences, and Engineering, University of Rochester, New York, 2015
7. <http://www.teledyne-si.com/ps-h4rg.html>.
8. <http://www.gaisler.com/index.php/products/processors/leon3>